

A. Poretti
T.A.G.M. Huisman
I. Scheer
E. Boltshauser



Joubert Syndrome and Related Disorders: Spectrum of Neuroimaging Findings in 75 Patients

SUMMARY: VH and MTS are the neuroimaging hallmarks of JSRD. We aimed to look at the full spectrum of neuroimaging findings in JSRD and reviewed the MR imaging of 75 patients with JSRD, including 13 siblings and 4 patients with OFD VI. All patients had VH and enlargement of the fourth ventricle. The degree of VH and the form of the MTS were variable. In most patients, the cerebellar hemispheres were normal and the PF was enlarged. Brain stem morphology was abnormal in 30% of the patients. Supratentorial findings included hippocampal malrotation, callosal dysgenesis, migration disorders, cephaloceles, and ventriculomegaly. All patients with OFD VI had a similar pattern, including HH in 2 patients. No neuroimaging-genotype correlation could be found. The wide neuroimaging spectrum in our patients supports the heterogeneity of JSRD. Neuroimaging differences in siblings represent intrafamilial heterogeneity. Due to the absence of a correlation with genotype, neuroimaging findings are of limited value in classifying patients with JSRD.

ABBREVIATIONS: CC = corpus callosum; HH = hypothalamic hamartoma; IF = interpeduncular fossa; JS = Joubert syndrome; JSRD = Joubert syndrome and related disorders; MTS = molar tooth sign; OFD VI = oral-facial-digital syndrome type VI; PF = posterior fossa; PMG = polymicrogyria; SCP = superior cerebellar peduncles; VH = vermian hypoplasia

JS is a rare syndrome characterized by hypotonia, ataxia, oculomotor apraxia, facial dysmorphism, and irregular neonatal breathing.¹⁻³ Cognitive functions are impaired in almost all patients. Based on the additional involvement of kidneys, liver, and/or eyes, 6 phenotypes of the JSRD spectrum have been defined.^{1,3} One phenotype corresponds to OFD VI syndrome. In OFD VI, tongue hamartomas and/or oral frenula and/or cleft palate, mesaxial polydactyly, and HH are associated features.³ To date, mutations in 10 genes have been associated with JSRD.³ Mutations in these genes account for less than 50% of the patients.³ The same gene can cause different phenotypes (allelic heterogeneity), and different genes can be associated with the same phenotype (locus heterogeneity).²

The neuroimaging hallmarks of JSRD include VH and the MTS. MTS results from a midbrain-hindbrain malformation characterized by thickened and elongated SCP and an abnormally deep IF.^{4,5} Although MTS and VH have been well described, few studies demonstrated their anatomic variability and additional infratentorial and supratentorial neuroimaging findings in JSRD.^{4,6,7}

The aim of this study was to extend and better characterize the spectrum of neuroimaging findings in the largest series of patients with JSRD reported so far, to our knowledge.

Materials and Methods

Neuroimaging data were collected by the senior author from the following sources: 1) his personal cohort of patients with JSRD diagnosed during a period of >30 years, 2) patients referred for a second opinion, and 3) requests to evaluate clinical and neuroimaging data of patients with a definite or probable diagnosis of JSRD. The inclusion criteria were the following: 1) availability of 1 MR imaging study of diagnostic quality including at least axial and sagittal T1- and T2-weighted MR images, 2) neuroimaging findings consistent with JSRD (MTS and VH), and 3) clinical findings compatible with JSRD. Seventy-five patients (52 males, 69%) fulfilled the inclusion criteria, including 13 siblings from 6 families and 4 patients with OFD VI and Meckel syndrome, respectively. In some of these patients, the genotype was known and included mutations in *AH11*, *CEP290*, *RPGRIPL1*, *TMEM67*, *INPP5E*, and *TMEM216* genes.

The diagnosis of OFD VI was indicated by the additional findings reported above. The diagnosis of Meckel syndrome was indicated by additional findings, including enlarged (polycystic) kidneys and a cephalocele.

All available images were retrospectively evaluated by 2 pediatric neurologists and 2 experienced pediatric neuroradiologists (T.A.G.M.H., I.S.) in consensus.

Infratentorial Image Analysis

The infratentorial anatomy was evaluated for qualitative assessment of the size (degree of hypoplasia) and morphology (normal/folial disorganization) of the vermis and hemispheres (normal or reduced or enlarged by visual evaluation). The extent of VH was graded according to Quisling et al.⁴ On sagittal images, the size and shape of the fourth ventricle were evaluated. On axial images, the shape of the interhemispheric cleft (linear, like an inverted Y) was assessed and its width was graded ("slit" if ≤ 1 , 1–2, or ≥ 2 mm).

The PF was qualitatively evaluated on sagittal images, including size (normal or enlarged), the presence of increased retrocerebellar CSF collection (present or marked, best assessed on axial images), and the size of the prepontine cistern (normal, enlarged if equal to or greater than twice the cross-sectional diameter of the basilar artery).

The SCP were evaluated on axial images for width (minimally or

Received October 8, 2010; accepted after revision December 17.

From the Divisions of Pediatric Neurology (A.P., E.B.) and Diagnostic Imaging (I.S.), University Children's Hospital of Zurich, Zurich, Switzerland; and Division of Pediatric Radiology (A.P., T.A.G.M.H.), Russell H. Morgan Department of Radiology and Radiological Science, The Johns Hopkins University School of Medicine, Baltimore, Maryland.

Dr Poretti was supported financially by the Swiss National Science Foundation.

Please address correspondence to Eugen Boltshauser, MD, Division of Pediatric Neurology, University Children's Hospital, Steinweiss 75, 8032 Zurich, Switzerland; e-mail: Eugen.Boltshauser@kispi.uzh.ch



Indicates article with supplemental on-line table.

<http://dx.doi.org/10.3174/ajnr.A2517>

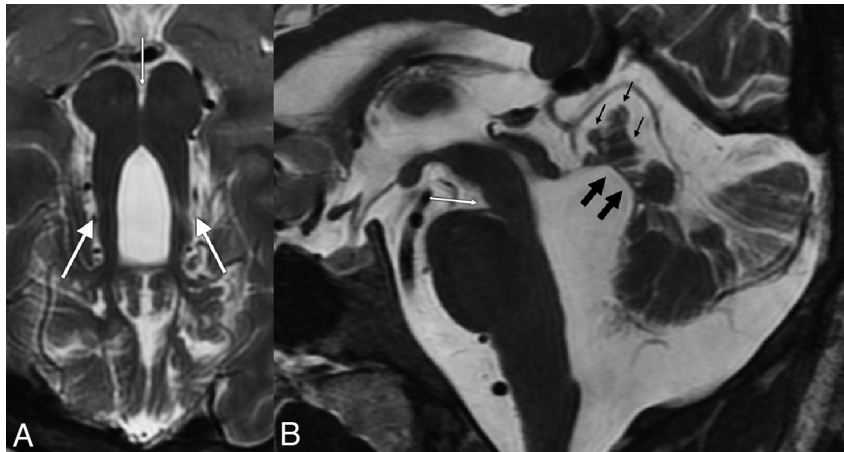


Fig 1. A, Axial T2-weighted MR image shows the classic MTS, including thickened, elongated, parallel, and horizontally orientated SCP (thick white arrows) and a deepened IF (thin white arrow). B, Midsagittal T2-weighted MR image demonstrates a severe vermian hypoplasia-dysplasia (thin black arrows), and distortion and enlargement of the fourth ventricle with rostral shifting of the fastigium (thick black arrows), enlargement of the PF, a deepened IF (white arrow), and a narrow pontomesencephalic isthmus.

obviously thickened), length (normal, very elongated if almost equally as long as the PF), and orientation (parallel, A-like, V-like, or curved). The depth of the IF was graded (minimally or obviously deepened). On axial images, the cerebral peduncles were evaluated for asymmetry.

The brain stem was assessed on sagittal images. The mesencephalon was evaluated regarding morphology (normal or dysmorphic), length (normal, shortened, or elongated), and width (normal, thin, or thickened). The presence of interpeduncular heterotopia lying anterior to or within the IF was ascertained. The morphology of the tectum, pons, and medulla (normal or dysmorphic), the width of the pons and medulla (normal, reduced, or enlarged), and the presence of a posterior medullary protuberance were studied.

Cephaloceles in 2 locations were evaluated (occipitally, at the level of the foramen magnum).

Supratentorial Image Analysis

The supratentorial evaluation included a search for migrational disorders, midline defects (agenesis or dysgenesis of the CC, absence of the septum pellucidum), hippocampal malrotation, ventriculomegaly (as an enlargement of the lateral ventricles without signs of increased intracranial pressure), and HH.

Results

MR Imaging

All patients underwent MR imaging at their local hospitals as part of their routine diagnostic work-up. At MR imaging, the median age of the patients was 1.3 years (range, 2 days to 27.6 years).

Because the patients with OFD VI appeared to have a similar neuroimaging pattern, we decided to study this group separately and formed 2 groups. The first group included all patients with JSRD without OFD VI ($n = 71$); the second group encompassed the patients with OFD VI ($n = 4$).

Infratentorial Findings ($n = 71$)

Most infratentorial findings are summarized in the On-line Table. Additionally, VH was marked in 53% of patients, moderate in 42%, and mild in 4%. The vermian remnants appeared dysplastic in all patients (Fig 1). VH resulted in distortion and enlargement of the fourth ventricle in all patients (Fig 1B).

Supratentorial Findings ($n = 71$)

Eleven patients had hippocampal malrotation (bilateral in 3 patients and unilateral in 8; in 1 patient, it was associated with callosal agenesis). The CC was dysgenetic in 6 patients (agenetic in 1). Absence of the septum pellucidum was associated with agenesis—severe hypoplasia of the CC in 2 patients. Occipital cephaloceles were detected in 8 patients, including all 4 with a Meckel-like phenotype. In 1 patient, the cephalocele was associated with PMG. Ventriculomegaly was found in 4 patients. Observed migrational disorders included periventricular nodular heterotopias in 2 patients, PMG in 1, and focal cortical dysplasia in 1.

Neuroimaging Findings in Patients with OFD VI ($n = 4$)

Infratentorial findings are summarized in the On-line Table. Additionally, in all patients, VH was marked and the vermian remnants appeared dysplastic (Fig 2). The brain stem was abnormal in all patients.

In 1 patient, an occipital cephalocele was present and was associated with bilateral occipital PMG. In another patient, a cephalocele was found at the level of the foramen magnum. PMG was detected in 3 patients; in 1, it was associated with periventricular heterotopias. HH (Fig 2), ventriculomegaly, and hippocampal malrotation were identified in 2 patients.

Intrafamilial Comparison

Comparing the neuroimaging findings among siblings, we found some intrafamilial similarities. None of the siblings showed supratentorial abnormalities, increased retrocerebellar collection of CSF, or anomalies of the pons or medulla. In all siblings, the cerebellar hemispheres were of equal size. However, there were differences regarding the size of the vermis and PF, morphology of the cerebellar hemispheres and tectum, orientation of the SCP, and depth of the IF. The presence of interpeduncular heterotopias also differed in 2 siblings.

Discussion

JS was originally described in 4 siblings with vermian agenesis presenting with episodic hyperpnoea, oculomotor apraxia,

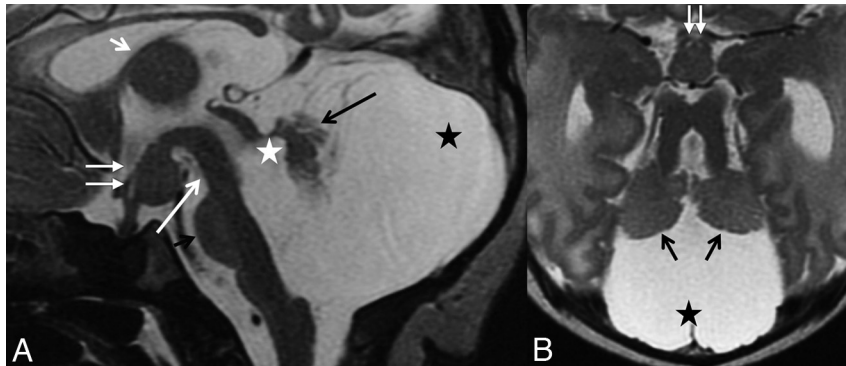


Fig 2. T2-weighted MR image of a 2-day-old patient with OFD VI. *A*, Midsagittal T2-weighted MR image shows a significant vermian hypoplasia-dysplasia of the vermis (*long black arrow*), an enlarged fourth ventricle (*white asterisk*), a PF with marked retrocerebellar CSF collection (*black asterisk*), and an HH (*white arrows*). In addition, the mesencephalon is elongated (*long white arrow*), the size of the pons is reduced (*short black arrow*), the CC is thin, and the interthalamic adhesion is enlarged (*short white arrow*). *B*, Axial T2-weighted MR image demonstrates hypoplasia of the vermis and both cerebellar hemispheres (*black arrows*), the characteristic MTS with thickened and elongated superior cerebellar peduncles, an abnormally deepened IF, an enlarged PF with marked retrocerebellar CSF collection (*black asterisk*), and an HH (*white arrows*). Modified with Permission from Poretti et al.¹⁵

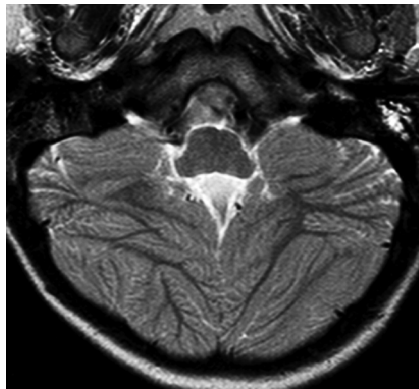


Fig 3. Axial T2-weighted MR image demonstrates a diffusely abnormal foliation and fissuration of both cerebellar hemispheres.

ataxia, and cognitive impairment.⁸ Maria et al⁹ reported the MTS as the characteristic neuroimaging finding of “pure” JS. However, the MTS is seen also in other syndromes.⁵ The term “JSRD” was coined to group all conditions sharing the MTS.³ MTS and VH resulting in distortion and enlargement of the fourth ventricle are consistent findings in JSRD.^{3,4,7} Therefore, MTS and VH are mandatory diagnostic criteria, and neuroimaging is essential for the diagnosis of JSRD.

JSRD is clinically heterogeneous. The different genes involved in JSRD can probably explain this marked pleiotropism. In a large cohort of patients with JSRD, we demonstrate the heterogeneity of neuroimaging findings. In previous reports, the size and morphology of the cerebellar hemispheres were reported as normal in almost all patients.^{4,7} Our study shows abnormal size and folial architecture in approximately one-quarter and more than one-third of patients, respectively (Fig 3). The size of the PF was variable, mimicking Dandy-Walker malformation if associated with an increased retrocerebellar CSF collection. The identification of an MTS is, however, essential for JSRD. The form of the MTS is also variable: the orientation of the SCP may differ (Fig 4), and the cerebral peduncles can be affected unequally, resulting in an asymmetric “crown” (Fig 5A). The deepening of the IF results from the absence of decussation of the SCP.¹⁰ It is unclear whether the minimal deepening of the IF in some of our patients may be related to a partial absence of the decussation. The brain stem

appeared dysmorphic in approximately 30% of patients.⁶ The mesencephalon and tectal plate were more frequently affected than the pons and medulla (Fig 5B).

Of special interest is the occurrence of nodular brain-isointense tissue between and in direct contact with the cerebral peduncles. On the basis of the isointensity to normal parenchyma and the location, Harting et al¹¹ called these “interpeduncular heterotopia.” We detected these in 3 patients with pure JS (no genetic data are available for these patients; 2 patients are included in Harting et al¹¹). Due to their location, the interpeduncular heterotopias should be distinguished from HH.

In our series, we found 2 forms and locations of cephaloceles. Occipital and atretic cephaloceles were detectable in 8 patients, including all with a Meckel-like phenotype. Both JSRD and Meckel syndrome are ciliopathies, and a significant overlap has been reported.¹² Of interest are small cephaloceles in the occipital bone at the level of the foramen magnum (Fig 6). These cephaloceles present as a diverticular meningeal protrusion filled with CSF. Only 1 case was previously illustrated by Doherty.¹ In accordance with the literature, our study showed that agenesis of the CC and hydrocephalus are exceptional findings in JSRD.^{13,14}

Both the clinical and prognostic significance and the pathogenesis of the neuroimaging heterogeneity in JSRD remain unclear. Because follow-up data are only available in a small proportion of patients, this study cannot resolve the question of the clinical and prognostic significance. The long-term clinical experience with patients with JSRD of the senior author (E.B.), however, does not support a prognostic role for neuroimaging in JSRD. Like the clinical heterogeneity, the neuroimaging variety in JSRD could be explained by the different genes involved. The involvement of the *AH11* gene in 2 families with PMG could suggest a neuroimaging-genotype correlation.¹⁵ Our study shows several differences when comparing MR images of siblings (intrafamilial variability). Additionally, in the patients with a known genotype, no distinct neuroimaging findings corresponding to the genetic background could be detected. Both observations do not support a neuroimaging-genotype correlation. The classification of patients with JSRD should be based on the organ involvement and the established correlation between genotype and clinical

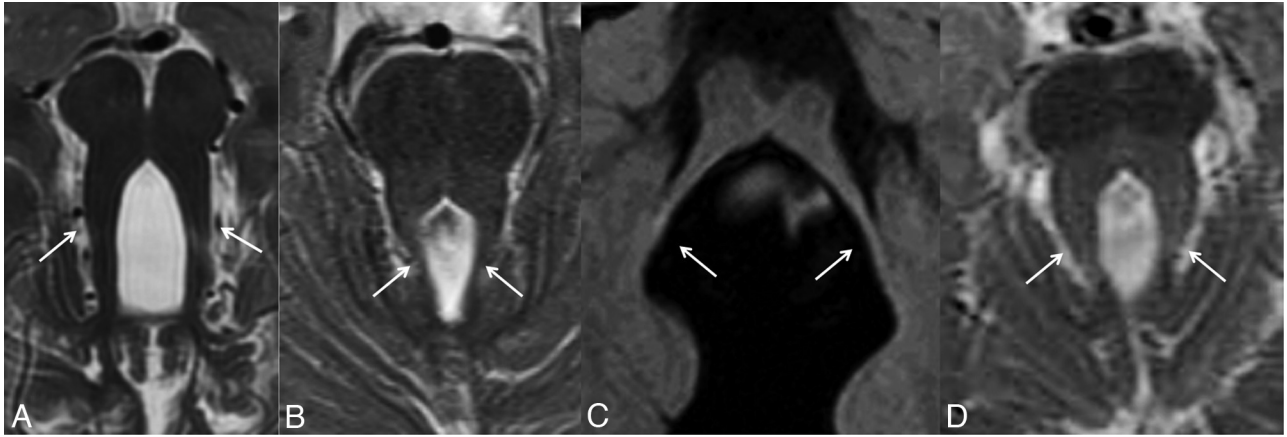


Fig 4. Axial T1- and T2-weighted images reveal parallel (A), V-like (B), A-like (C), and curved (D) SCP orientations (white arrows).

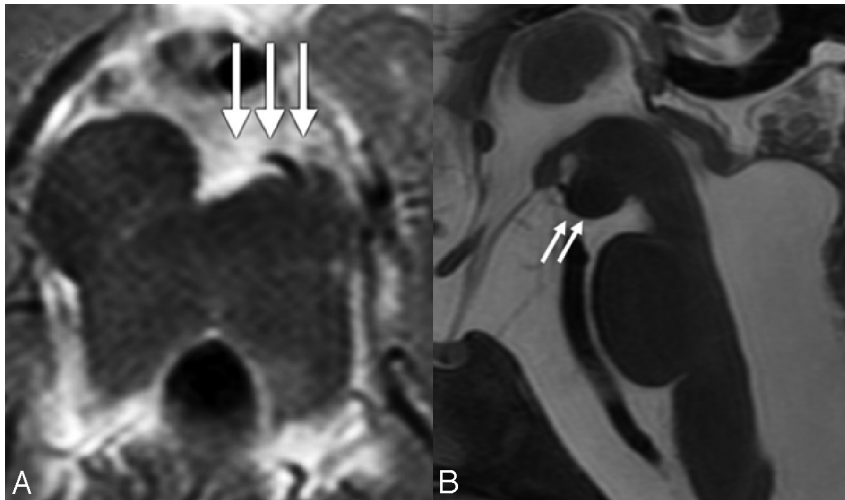


Fig 5. A, Axial T2-weighted MR image shows asymmetry of the cerebral peduncles, giving them an appearance of a decaying molar tooth on axial images (white arrows). B, Midsagittal T2-weighted MR image reveals a dysmorphic mesencephalon (white arrows) and an enlarged prepontine cistern with increased vertical orientation of the brain stem.

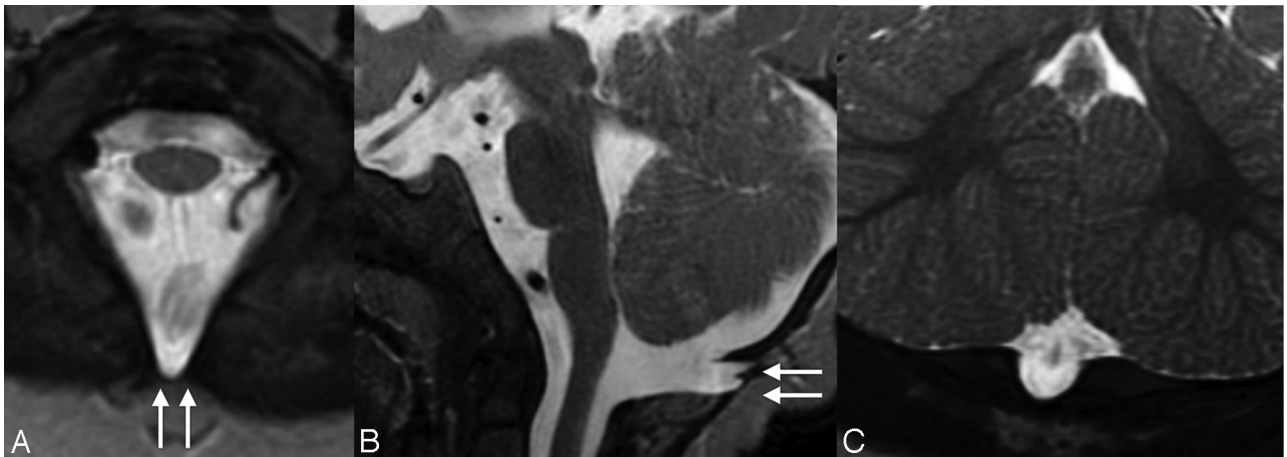


Fig 6. Axial (A), midsagittal (B), and coronal (C) T2-weighted MR images show a protrusion of the meninges through a fissure in the dorsal bony margin of the foramen magnum, representing a cephalocele (white arrows).

phenotype.³ The neuroimaging spectrum associated with mutations in the same gene (allelic heterogeneity) could be related to the presence of genetic-epigenetic modifiers of the phenotype that are still unknown.^{1,2}

Only the 4 patients with OFD VI showed similar (more

severe) neuroimaging findings, including severe VH, enlargement of the PF, hypoplastic and dysplastic cerebellar hemispheres, increased retrocerebellar CSF collection, and an abnormal brain stem. Supratentorial abnormalities appeared more frequently in patients with OFD VI. HH is not patho-

gnomonic but characteristic for OFD VI.^{5,16,17} The association of MTS, HH, and pronounced neuroimaging findings suggests the diagnosis of OFD VI. This represents the only pattern suggesting the classification of patients with JSRD based on neuroimaging that has clinical and prognostic significance. Patients with OFD VI have, overall, a significantly more severe neurologic and cognitive impairment than most patients with JSRD. Two of our patients died in infancy, and the 2 survivors have very severe neurologic and cognitive impairments (no ambulation, no expressive language).

We are aware of the limitations in our study: The evaluation includes only qualitative, not quantitative measures; the MR imaging examinations were performed in different hospitals with different protocols; data about clinical follow-up and genetic background are unavailable for a considerable proportion of patients; and the group of patients with OFD VI is too small to define a consistently pathognomonic neuroimaging pattern. However, we believe that presenting the largest cohort of patients with JSRD that could be studied strengthens the data validity.

Conclusions

This study reveals a wide spectrum of neuroimaging findings in JSRD. Although further studies in large cohorts of patients with JSRD with known mutations are needed to search for a neuroimaging-genotype correlation, this study confirms the heterogeneity in JSRD, not only from the clinical and neurogenetic but also from the neuroimaging point of view. Variable findings in affected siblings support the intrafamilial heterogeneity in JSRD. Patients with OFD VI share a similar more severe neuroimaging pattern.

Acknowledgments

We thank all colleagues for sharing neuroimaging data of patients with JSRD. In particular, we acknowledge Dan Doherty, MD,

PhD, Children's Hospital of Seattle, and Inga Harting, MD, University Hospital of Heidelberg, for helpful discussions.

References

1. Doherty D. **Joubert syndrome: insights into brain development, cilium biology, and complex disease.** *Semin Pediatr Neurol* 2009;16:143–54
2. Parisi MA. **Clinical and molecular features of Joubert syndrome and related disorders.** *Am J Med Genet C Semin Med Genet* 2009;151C:326–40
3. Brancati F, Dallapiccola B, Valente EM. **Joubert syndrome and related disorders.** *Orphanet J Rare Dis* 2010;5:20
4. Quisling RG, Barkovich AJ, Maria BL. **Magnetic resonance imaging features and classification of central nervous system malformations in Joubert syndrome.** *J Child Neurol* 1999;14:628–35, discussion 69–72
5. Gleeson JG, Keeler LC, Parisi MA, et al. **Molar tooth sign of the midbrain-hindbrain junction: occurrence in multiple distinct syndromes.** *Am J Med Genet A* 2004;125A:125–34, discussion 17
6. Alorainy IA, Sabir S, Seidahmed MZ, et al. **Brain stem and cerebellar findings in Joubert syndrome.** *J Comput Assist Tomogr* 2006;30:116–21
7. Senocak EU, Oguz KK, Haliloglu G, et al. **Structural abnormalities of the brain other than molar tooth sign in Joubert syndrome-related disorders.** *Diagn Interv Radiol* 2010;16:3–6
8. Joubert M, Eisenring JJ, Robb JP, et al. **Familial agenesis of the cerebellar vermis: a syndrome of episodic hyperpnea, abnormal eye movements, ataxia, and retardation.** *Neurology* 1969;19:813–25
9. Maria BL, Hoang KB, Tusa RJ, et al. **“Joubert syndrome” revisited: key ocular motor signs with magnetic resonance imaging correlation.** *J Child Neurol* 1997;12:423–30
10. Poretti A, Boltshauser E, Loenneker T, et al. **Diffusion tensor imaging in Joubert syndrome.** *AJNR Am J Neuroradiol* 2007;28:1929–33
11. Harting I, Kotzaeridou U, Poretti A, et al. **Interpeduncular heterotopia in Joubert syndrome: a previously undescribed MR finding.** *AJNR Am J Neuroradiol* 2011;32:1286–89
12. Boycott KM, Parboosingh JS, Scott JN, et al. **Meckel syndrome in the Hutterite population is actually a Joubert-related cerebello-oculo-renal syndrome.** *Am J Med Genet A* 2007;143A:1715–25
13. Zamponi N, Rossi B, Messori A, et al. **Joubert syndrome with associated corpus callosum agenesis.** *Eur J Paediatr Neurol* 2002;6:63–66
14. Anderson JS, Gorey MT, Pasternak JF, et al. **Joubert's syndrome and prenatal hydrocephalus.** *Pediatr Neurol* 1999;20:403–05
15. Dixon-Salazar T, Silhavy JL, Marsh SE, et al. **Mutations in the AHI1 gene, encoding joubertin, cause Joubert syndrome with cortical polymicrogyria.** *Am J Hum Genet* 2004;75:979–87. Epub 2004 Oct 4
16. Stephan MJ, Brooks KL, Moore DC, et al. **Hypothalamic hamartoma in oral-facial-digital syndrome type VI (Varadi syndrome).** *Am J Med Genet* 1994;51:131–36
17. Poretti A, Brehmer U, Scheer I, et al. **Prenatal and neonatal MR imaging findings in oral-facial-digital syndrome type VI.** *AJNR Am J Neuroradiol* 2008;29:1090–91